

Propellant-free Attitude Control for Spinning Solar Sail via Optical Parameter Switching

Ryu Funase,^{*1} Yuya Mimasu,^{*1} Yuichi Tsuda,^{*1} Takanao Saiki,^{*1}
Yoshinobu Okano^{*2} and Go Kanno^{*3}

*1: Japan Aerospace Exploration Agency, Japan

*2: Tokyo Metropolitan University, Japan

*3: Tokai University, Japan

A fuel-free attitude control system for a spinning solar sail which utilizes solar radiation pressure was developed. This system consists of thin-film devices attached to the sail that electrically control their optical parameters such as reflectivity, and the attitude control torque is generated by switching their optical parameters synchronizing with spin motion. Attitude control torque model for a sail of arbitrary shape and deformation was derived. The control system was implemented for Japanese interplanetary solar sail demonstration spacecraft IKAROS and the on-orbit attitude control performance was evaluated.

セイルの光学パラメータ切り替え制御による スピン型ソーラーセイルの燃料フリー姿勢制御

本論文では、スピン型ソーラーセイルの燃料フリー姿勢制御系の設計と、ソーラー電力セイル実証機 IKAROS での飛翔結果を示す。大面積の薄膜(セイル)を有するスピン型ソーラーセイルに、反射特性を電氣的に制御可能な姿勢制御デバイスを実装し、太陽光圧のアンバランスによって姿勢制御トルクを発生させる燃料フリー姿勢制御系を開発し、小型ソーラー電力セイル実証機 IKAROS に搭載した。任意の変形を有するソーラーセイルを前提とし、提案する姿勢制御系の姿勢運動モデルや姿勢制御性能について導出した。最後に本姿勢制御システムの IKAROS での飛翔結果について示す。

INTRODUCTION

A solar sail, which consists of a huge and thin membrane deployed in space that acquires propulsive force by the reflection of sunlight, is considered to be one of the most essential propulsion systems for future solar system exploration. This is because solar photon propulsion does not require any consumable propellant. Thus, it can enable farther and longer space travel compared with a conventional propulsion system whose acceleration limit is determined by the amount of propellant. Although the acceleration obtained by sunlight reflection is very small, the total increase in velocity will become large if this acceleration is accumu-

lated 24 hours a day, every day.

Numerous organizations such as those in Japan (JAXA), the United States of America (NASA and/or the Planetary Society), and Europe (ESA) have been studying various types of solar sails. There are two main types of solar sails: rigid-type solar sails and spin-type solar sails. The rigid type [1] is a solar sail with a rigid structure such as masts to deploy and support the flexible membrane (Figure 1). The spin type is a solar sail without a rigid support structure, where the sail membrane is attached to the center spacecraft hub and is deployed and extended using the centrifugal force of the spin motion (Figure 2). JAXA originally pro-



Figure 1. Rigid type solar sail studied in NASA.

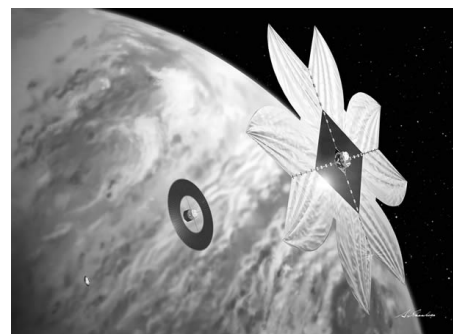


Figure 2. Spin type solar sail studied in JAXA.

posed this type of solar sail [2].

The spin-type solar sail can approximate an ideal solar photon sail because of its potential to realize almost the same weight/area ratio (or acceleration) as the thin-film membrane material. However, it has some disadvantages in terms of attitude control. First, its attitude motion is complicated because of the flexibility of the membrane which does not have any support structure but relies on the centrifugal force for its shape maintenance. Impulsive torque input by conventional chemical thrusters will induce oscillatory motion in the membrane. Second, in terms of the propellant consumption for attitude control (or steering of the sail) which is necessary for orbital control, the spin type has to change the orientation of the large angular momentum of the large spinning membrane for its orbital control. In some cases, the amount of propellant may limit the lifetime of the spinning solar sail. On the other hand, it also has some advantages in attitude stability or operation safety. Detailed discussions are described in our previous work [3]. With these trade-offs, an attitude control system that does not induce oscillation in the flexible membrane and does not consume much propellant for attitude control will extend the potential/applicability of the spin-type sail. This will lead to an ideal lightweight solar photon sail with the theoretical maximum acceleration, which is the intrinsic advantage of the spin-type solar sail.

The authors had proposed a propellant-free and oscillation-free attitude control system for spinning solar sails that utilize only the solar radiation pressure and solar energy [3]. In this system, a number of specially developed thin-film reflectivity control devices (RCD) that can electrically control their optical parameters are attached to the sail membrane, and attitude control torque can be generated by changing the reflectivity of these devices to generate an imbalance in the solar radiation pressure applied to the sail. This system can generate minute and continuous control torque input, preventing it from exciting unnecessary oscillations. Moreover, this control system does not consume any propellant. The control system was implemented as an optional attitude control system for small solar power sail demonstrator named IKAROS (Interplanetary Kite-craft Accelerated by Radiation Of the Sun) [4]. In-orbit attitude control experiments were conducted, and the normal operation of the control system was confirmed by the initial flight results of IKAROS [3].

In this paper, the authors developed a practical three-dimensional attitude control torque model of the system which can incorporate arbitrary defor-

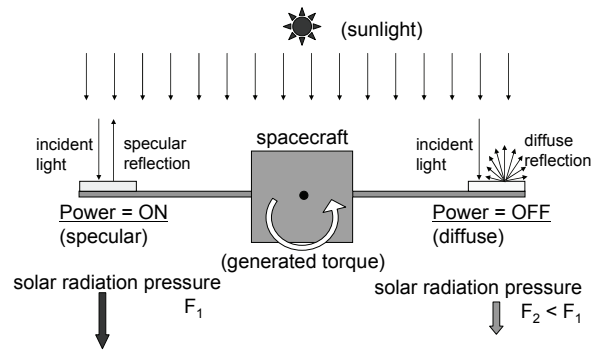


Figure 3. Concept of proposed attitude control system using only solar radiation pressure.

mation of solar sail membrane, while the previously-developed simplified model assumed completely flat sail membrane and that the attitude control torque was generated by one-dimensional solar radiation pressure perpendicular to the flat surface [3]. The on-orbit attitude control results were discussed by comparing with the improved torque model, and the performance of the proposed control system and the deformation of sail membrane was investigated.

This paper is organized as follows. First, the proposed propellant-free (and oscillation-free) attitude control system for spinning solar sails and the specially developed RCD is briefly introduced. Next, the improved three-dimensional attitude control torque model for this control system is developed. The effect of sail deformation on the control performance is incorporated in the model. Finally, the on-orbit attitude control experiment results are shown and discussed.

PROPELLANT-FREE ATTITUDE CONTROL OF SPINNING SOLAR SAIL

Concept of the Control System

Figure 3 shows the concept of the attitude control system which utilizes the solar radiation pressure. In this system, a number of devices that can control their optical parameters such as specular/diffuse reflectivity are attached to the edge of the sail membrane. Thus, attitude control torque can be generated by changing the reflectivity of these devices to generate an imbalance in the solar radiation pressure applied to the edge of the sail. This system can generate minute and continuous control torque input, preventing it from exciting unnecessary oscillations. Moreover, this control system does not consume any propellant.

RCD

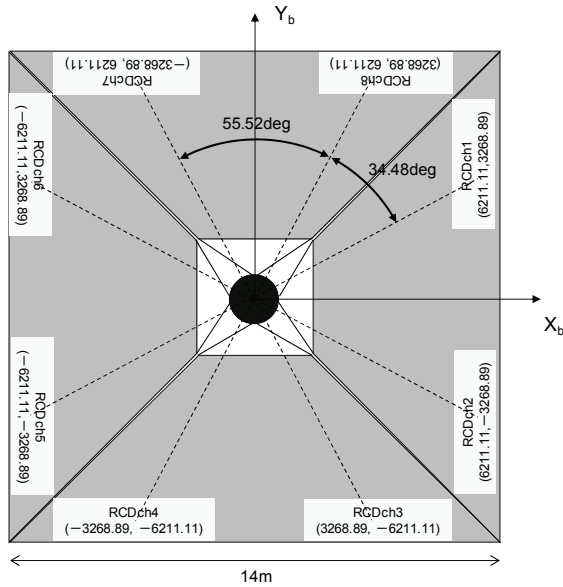


Figure 4. Arrangement of eight blocks of RCDs on IKAROS' sail. The value in brackets indicate the coordinate of each blocks in the body-fixed coordinate system.

RCD was developed as a key component to realize this control system. The RCD is a thin film device that can control the orientation of liquid crystal components sandwiched between two electrodes by applying appropriate voltages to the electrodes. Based on the light control glasses used commercially on the ground which can switch between diffuse transmission and regular transmission, a thin-film radiation tolerant RCD was developed for a spin-type solar sail. [3] This RCD can switch between specular reflection and diffuse reflection just by electric power.

This system was implemented as an optional attitude control system for JAXA's small solar power sail demonstrator IKAROS, which was launched in May 2010. Figure 4 shows where the devices were attached to the sail of IKAROS. A total of 72 devices (25 cm × 1 m × 70 μm thick sheets) were attached to the outer edges of the 14 m × 14 m square solar sail membrane. Attitude control is performed by supplying electric power from the center spacecraft, therefore this system does not consume any propellant.

The most significant point of this method other than the fuel-free feature is that a small and continuous control torque is applied directly to the sail which constitutes the majority of the large angular momentum of the spinning solar sail. This leads to a smaller oscillation of the membrane or smaller nutation of the center spacecraft. If conventional chemical thrusters on the small center spacecraft are used for attitude control, large attitude maneuver of the center spacecraft is required in order to

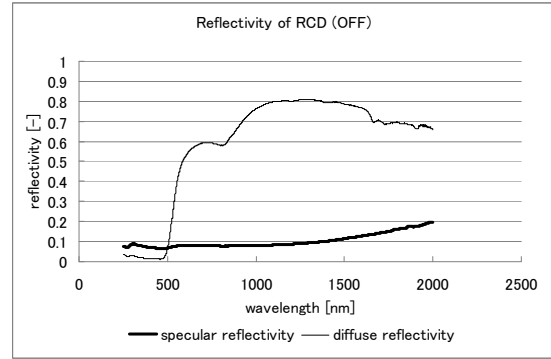


Figure 5. Reflectivity of RCD when it is OFF.

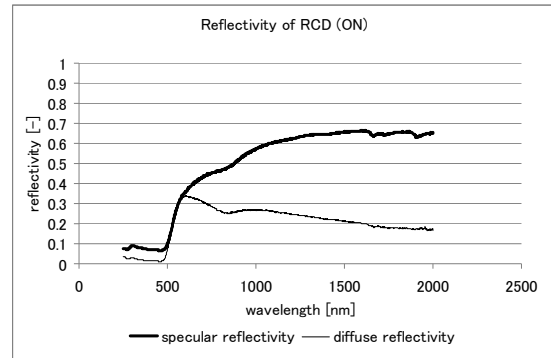


Figure 6. Reflectivity of RCD when it is ON.

realize reorientation of the large angular momentum of the sail, even if the reorientation angle is small. The sail with the majority of the large angular momentum does not quickly follow the attitude motion of the center spacecraft, and this large angular difference between the sail and the spacecraft will result in unnecessary oscillation of the membrane and the oscillation will continue for a long time until the damping effect in the membrane dissipates the oscillation energy.

The optical parameters of RCD were measured using a spectrometer. Figures 5 and 6 show the reflectivity of RCD for the light of wavelength from 250 nm to 2000 nm when it is OFF and ON, respectively. Effective specular/diffuse reflectivity for the sunlight were obtained by multiplying these measurement results by the sun light intensity profile and integrating for overall effective range of wavelength. Table. 1 shows the optical performance and other related parameters of IKAROS' RCD.

Table 1. Optical performance and other parameters of IKAROS' RCD.

Parameter	Value	Unit
$C_{s_{on}}$	0.38	-
$C_{d_{on}}$	0.20	-
$C_{a_{on}}$	0.42	-

$C_{s_{off}}$	0.08	-
$C_{d_{off}}$	0.47	-
$C_{a_{off}}$	0.45	-
ΔC_s	0.30	-
ΔC_d	-0.27	-
A	12.6	m ²
R	7.02	m

ATTITUDE CONTROL TORQUE MODEL

Coordinate System Definition and Basic Equations

In this section, attitude control torque generated by the proposed control system is analytically modeled. The previously developed model [3] assumed that all devices were attached to completely flat sail membrane and that the attitude control torque was generated by one-dimensional solar radiation pressure perpendicular to the flat surface. However, the shape of the sail can be deformed by the solar radiation pressure, as is actually observed for IKAROS (see Figure 11). Thus, the improved model incorporated three dimensional components of solar radiation pressure vector applied to each device attached to arbitrarily deformed solar sail membrane.

We consider a coordinate system where the spin axis of the solar sail is in z-axis and the sun direction vector \vec{s} is in x-z plane whose x component is positive (Figure 7). The origin of the coordinate system is center of gravity of overall spacecraft hub and the sail. The attitude control torque is expressed in this inertial spin-free coordinate system.

Here, we suppose a single RCD element with area A is located at $\vec{r} = [R, 0, h] = R[1, 0, h']$ in the coordinate system and the element's surface normal

vector is tilted toward x-direction by angle α and toward y-direction by angle β . The angle α , β and the vertical offset h represents non-flat property of the sail (or RCD). α and β correspond to radial deformation (deflection) and circumferential deformation (distortion) respectively. These non-flat property can exist when the sail is deformed due to solar radiation pressure.

The RCD's normal vector varies during a spin motion as a function of the spin phase θ :

$$\vec{n} = \begin{bmatrix} \cos \theta & -\sin \theta & 0 \\ \sin \theta & \cos \theta & 0 \\ 0 & 0 & 1 \end{bmatrix} \begin{bmatrix} \sin \alpha \\ \cos \alpha \sin \beta \\ \cos \alpha \cos \beta \end{bmatrix} \quad (1)$$

This means that the surface normal vector of RCD varies as the RCD rotates around the z-axis. Note that the vector is constant $([0,0,1])$ for a perfectly flat sail.

The force applied to the RCD by solar radiation pressure is described using optical property of RCD and other parameters as the following equation:

$$\vec{F} = -p_0 A (\vec{n} \cdot \vec{s}) \left[(1 - C_s) \vec{s} + \{2C_s (\vec{n} \cdot \vec{s}) + B_f C_d\} \vec{n} \right] \quad (2)$$

B_f is Lambertian coefficient which is related to how the light from diffuse reflection is hemispherically uniform. B_f is equal to 2/3 for perfectly uniform diffuse property. The sun direction vector \vec{s} is $[\sin \theta_s, 0, \cos \theta_s]$, which is independent of the spin phase θ . Only the force by optical reflection and absorption is considered in Eq. (2) and transparency of the device is assumed to be 0. The force by thermal radiation is not considered.

Let us put an approximation hereafter that the angle α , β , θ_s and the normalized vertical offset h' are sufficiently small, then the following equations hold by considering up to second-order terms.

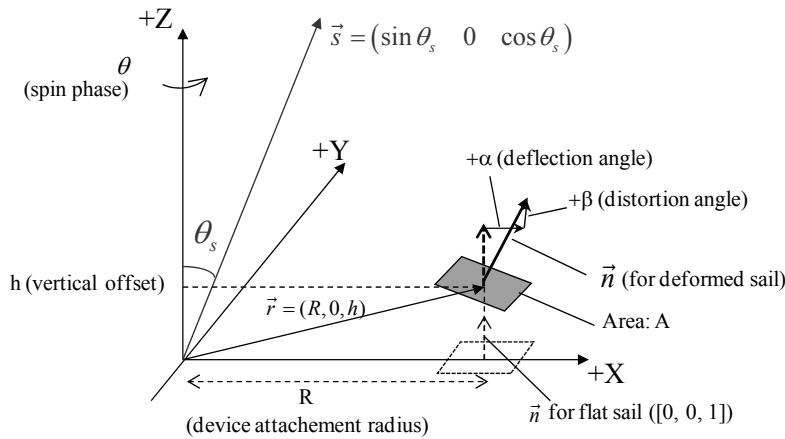


Figure 7. Definition of coordinate system and sail deformation.

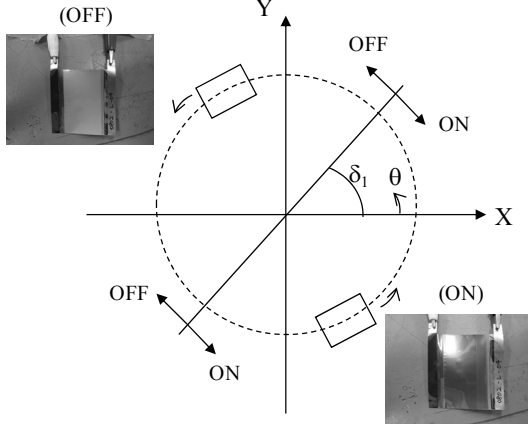


Figure 8. Definition of switching control scheme and switching phase δ_1 .

$$\vec{n} \cong \begin{bmatrix} \alpha \cos \theta - \beta \sin \theta \\ \alpha \sin \theta + \beta \cos \theta \\ 1 - \frac{\alpha^2 + \beta^2}{2} \end{bmatrix} \quad (3)$$

$$\vec{s} \cong \begin{bmatrix} \theta_s & 0 & 1 - \frac{\theta_s^2}{2} \end{bmatrix} \quad (4)$$

$$\vec{n} \cdot \vec{s} \cong (\alpha \cos \theta - \beta \sin \theta) \theta_s + 1 - \frac{\alpha^2 + \beta^2 + \theta_s^2}{2} \quad (5)$$

Then, the force applied to the RCD by solar radiation pressure in Eq. (2) can be approximated as

$$\frac{\vec{F}}{p_0 A} \cong \begin{bmatrix} (2C_s + B_f C_d)(\beta \sin \theta - \alpha \cos \theta) + (C_s - 1)\theta_s, \\ -(2C_s + B_f C_d)(\alpha \sin \theta + \beta \cos \theta), \\ (B_f C_d + 1)\beta \theta_s \sin \theta - (3C_s + B_f C_d + 1)\alpha \theta_s \cos \theta + (C_s + \frac{1}{2} B_f C_d + 1)\theta_s^2 \\ + (\frac{5}{2}\alpha^2 + \frac{5}{2}\beta^2 - 1)C_s + (\alpha^2 + \beta^2 - 1)B_f C_d + \frac{1}{2}\alpha^2 + \frac{1}{2}\beta^2 - 1 \end{bmatrix} \quad (6)$$

Attitude Control Torque by RCD Switching Control

Using above equation, attitude angular momentum is accumulated by switching the RCD in synchronization with the spin motion. Here, we assume that the RCD is turned off for $\delta_1 \leq \theta \leq \delta_1 + \pi$ and turned on for $\delta_1 + \pi \leq \theta \leq \delta_1 + 2\pi$ (Figure 8).

Then, the attitude angular momentum generated by the control for one spin motion is calculated as the following equation:

$$\begin{aligned} \Delta L &= L_{control} - L_{no_control} \\ &= \int_{\theta=\delta_1+\pi}^{\theta=\delta_1+2\pi} \vec{r} \times (\vec{F}_{ON} - \vec{F}_{OFF}) dt \quad (7) \\ &= \frac{1}{\Omega} \int_{\theta=\delta_1+\pi}^{\theta=\delta_1+2\pi} (\vec{r} \times \vec{F}_{ON} - \vec{r} \times \vec{F}_{OFF}) d\theta \end{aligned}$$

The first term of the integration is the angular momentum generated by RCD switching control for $\delta_1 \leq \theta \leq \delta_1 + \pi$ and the second term is the angular momentum generated by RCD when it is always OFF (no control), and the attitude angular momentum generated by the RCD switching control is the difference between these two integrations. The calculation of F_{OFF} is based on the optical parameters when the RCD is off ($C_{s_{off}}$ and $C_{d_{off}}$) and F_{ON} is based on $C_{s_{on}}$ and $C_{d_{on}}$ in Table. 1. Each components of the angular momentum vector ΔL are calculated as follows:

$$\begin{aligned} \frac{\Delta L_x}{p_0 R A / \Omega} &= \frac{1}{2} \left[-(4\Delta C_s + 2B_f \Delta C_d) \theta_s^2 \cos \delta_1 + \pi B_f \Delta C_d \beta \theta_s + (4\Delta C_s + 4B_f \Delta C_d) \cos \delta_1 \right. \\ &\quad \left. - (8\Delta C_s + 4B_f \Delta C_d) (\alpha \cos \delta_1 - \beta \sin \delta_1) h' - (\alpha^2 + \beta^2) (10\Delta C_s + 4B_f \Delta C_d) \cos \delta_1 \right] \quad (8) \end{aligned}$$

$$\begin{aligned} \frac{\Delta L_y}{p_0 R A / \Omega} &= \frac{1}{2} \left[-(4\Delta C_s + 2B_f \Delta C_d) \theta_s^2 \sin \delta_1 + \pi (2\Delta C_s h' + \alpha (3\Delta C_s + B_f \Delta C_d)) \theta_s + (4\Delta C_s + 4B_f \Delta C_d) \sin \delta_1 \right. \\ &\quad \left. - (8\Delta C_s + 4B_f \Delta C_d) (\alpha \sin \delta_1 + \beta \cos \delta_1) h' - (\alpha^2 + \beta^2) (10\Delta C_s + 4B_f \Delta C_d) \sin \delta_1 \right] \quad (9) \end{aligned}$$

$$\frac{\Delta L_z}{p_0 R A / \Omega} = 2\Delta C_s \theta_s \cos \delta_1 - \pi (2\Delta C_s + B_f \Delta C_d) \beta \quad (10)$$

Special Case ($\delta_1=0$)

Here, we consider a special switching control sequence of $\delta_1 = 0$. This sequence is optimum for generating sun pointing control torque in the +x direction when the sail is perfectly flat. In this case, the angular momentum ΔL_x , ΔL_y and ΔL_z is simplified as follows:

$$\begin{aligned} \frac{\Delta L_x}{p_0 R A / \Omega} &= \frac{1}{2} \left[-(4\Delta C_s + 2B_f \Delta C_d) \theta_s^2 + \pi B_f \Delta C_d \beta \theta_s + (4\Delta C_s + 4B_f \Delta C_d) \right. \\ &\quad \left. - (8\Delta C_s + 4B_f \Delta C_d) \alpha h' - (\alpha^2 + \beta^2) (10\Delta C_s + 4B_f \Delta C_d) \right] \quad (11) \end{aligned}$$

$$\frac{\Delta L_y}{p_0 R A / \Omega} = \pi \left\{ \Delta C_s h' + \frac{1}{2} \alpha (3\Delta C_s + B_f \Delta C_d) \right\} \theta_s - (4\Delta C_s + 2B_f \Delta C_d) \beta h' \quad (12)$$

$$\frac{\Delta L_z}{p_0 R A / \Omega} = 2\Delta C_s \theta_s - \pi (2\Delta C_s + B_f \Delta C_d) \beta \quad (13)$$

FLIGHT RESULTS

The proposed attitude control system using RCD was implemented as an optional attitude control system for IKAROS. IKAROS was launched on May 21st, 2010 and its solar sail was successfully deployed on June 10th. After the deployment of the sail, the main mission of IKAROS (acceleration by solar radiation pressure) was also successful [4]. This became the world's first solar sail demonstrated on orbit.

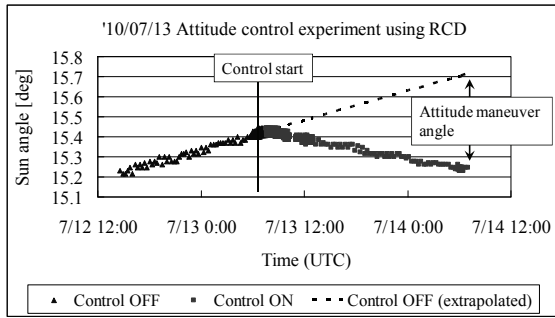


Figure 9. Sun-pointing attitude control result.

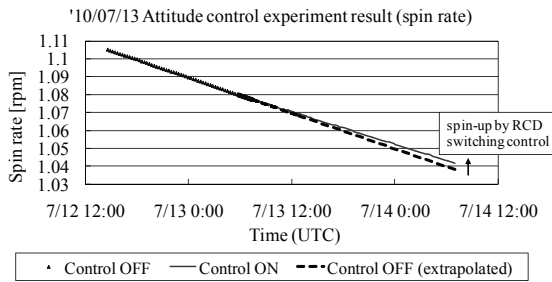


Figure 10. Spin rate history in the control experiment.

The first on-orbit control experiment was conducted on July 13th. In this experiment, attitude control was performed for 23 hours, or nearly a whole day. Spin axis precession torque was generated in the sun-pointing direction, allowing the attitude maneuver performance to be simply measured using the telemetry of the fine sun angle sensor. 8 blocks of RCDs (Figure 4) were switched ON and OFF in synchronization with the spin motion to generate attitude control torque in the fixed direction in the inertial coordinate system. In order to achieve this control logic, the onboard controller received a pulse signal from a slit-type sun sensor every spin motion, allowing it to calculate the spin period and timing of the ON and OFF states for each blocks of RCDs.

Figure 9 shows the attitude control result in terms of sun angle. The horizontal axis shows the time, and the vertical axis is the sun angle. The triangle dots in the left half represent the sun angle history before control, where the sun angle is slightly increasing because of the attitude drift motion. Attitude drift motion is a phenomenon that is observed for a interplanetary probe with angular momentum and the motion is produced by solar radiation pressure. This phenomenon occurs for a sail with deformation α , β and/or vertical offset h .

When the attitude control experiment started at 7:35 UTC on July 13th, the drift motion was suppressed by the maneuvering torque by the RCDs and the sun angle began to decrease (square dots). If the sun angle history before the control is ex-

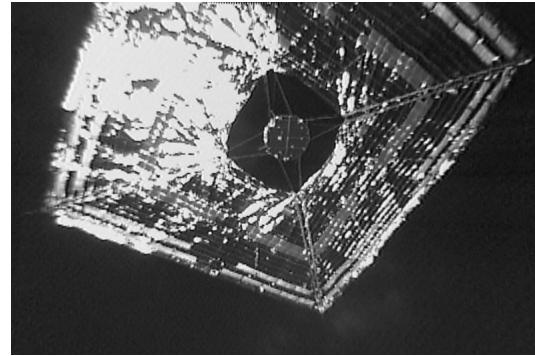


Figure 11. An example of obtained image of the deployed sail. RCD is attached on the edge of the sail. This image was obtained by a small camera-carrying probe deployed from the

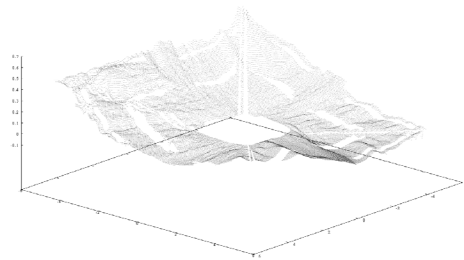


Figure 12. Preliminary result of sail shape estimation from a camera image.

trapolated (dashed line), the difference from the actual sun angle history after the control represents the attitude maneuver angle achieved by the RCDs. This experiment achieved an attitude control torque of 9.56×10^{-6} [Nms]. This performance is about 80% of performance estimation for completely flat sail ($\alpha=\beta=0$).

This attitude performance "degradation" is considered to be due to the sail deflection α and distortion β . Distortion angle β is closely related to the spin up/down torque (see Eq.(13)) and the information on spin up/down torque is provided by spin rate history before and during the control experiment. Figure 10 shows the spin rate telemetry around the control experiment. The spin rate is decreasing before and during the control experiment and this "acceleration" in the spin down direction decreases during the experiment. This means that a certain spin up torque was generated by the switching control of RCD. Figure 10 indicates that the spin up torque increase by the switching control is 3.85×10^{-6} [Nms], and Eq.(13) leads to the estimation of distortion angle to be about +4 [deg] .

Then, deflection angle α was estimated from the observed attitude maneuver torque. Based on the distortion angle estimation, the attitude maneuver torque can be described as a function of deflec-

tion angle (Eq.(11)), and the result implies the deflection angle is about -11 [deg]. These estimations is qualitatively consistent with the analysis of sail deformation based on camera images [5]. Figure 11 is an example of obtained camera images [6] and Figure 12 shows preliminary analysis of the sail shape [5]. These figures implies small negative deflection angle and positive distortion angle on average, which is consistent with the above estimation of α and β .

It should be noted that the above discussion on the sail deformation assumes nominal optical performance of RCD in Table. 1. The result of about 80% performance also implies the possibility that the on-orbit optical property of RCD is not exactly equal to that of Table 1. Independent and simultaneous estimation of both sail deformation and on-orbit optical performance of RCD will be possible by using multiple control experiment results under different condition of θ_s and RCD switching phase δ_1 . This analysis is left for further study.

In any case, the RCD itself showed the performance at least 80% of design value. Moreover, no nutation velocity excitation was observed during the control experiment. Therefore, it can be said that the goal of this control system, that is, stable and fuel-free attitude control of a spinning solar sail, was successfully achieved.

CONCLUSIONS

The authors proposed a new oscillation-free and fuel-free attitude control system for a spinning solar sail which utilizes solar radiation pressure. In order to realize such a stable and fuel-free attitude control of a flexible spinning solar sail, a thin-film RCD was specially developed. This device is capable of electrically controlling its optical properties. Using a number of such devices, attitude control can be performed by inducing an imbalance in the solar radiation pressure applied to the sail. The proposed control system was implemented as an optional attitude control system for IKAROS mission, and the normal operation of the control system was confirmed by the initial flight results.

In this paper, the authors developed a practical attitude control torque model of the system and the performance of the control system was rigorously discussed. The previously developed model assumed that all devices were attached to completely flat sail membrane and that the attitude control torque was generated by one-dimensional solar radiation pressure perpendicular to the flat surface. However, the shape of the sail can be deformed by the solar radiation pressure, as is actually observed for IKAROS. Thus, the improved model incorpo-

rated three dimensional components of solar radiation pressure vector applied to each devices attached to arbitrarily deformed solar sail membrane. The derived torque model can be seen as an extension of a solar radiation pressure model for normal spinning solar sail [7] in that our spin-averaged model incorporates time-varying optical parameter distribution (due to the switching control of optical property), while the model for normal spinning sail [7] imposes a circumferentially not-uniform but time-invariant optical parameter distribution.

Based on the improved attitude control torque model, the on-orbit attitude control experiment results were analyzed and almost full control performance was confirmed. The small degradation of the performance is considered to be partially due to sail deformation, which is consistent with the implication of camera image analysis. Detailed analysis of sail deformation and on-orbit optical performance of RCD is left for further study.

The proposed control system solves the two major challenges in the use of a spinning solar sail: the complicated attitude motion caused by the flexibility of the membrane and the large angular momentum to be handled by the attitude controller. This control system can contribute to the realization of an ideal solar photon propulsion system with the theoretical maximum weight/area ratio (or acceleration), which is the intrinsic advantage of a lightweight spinning solar sail.

NOTATION

C_s	specular reflectivity
C_d	diffuse reflectivity
C_a	absorptivity
ΔC_s	specular reflectivity difference between ON and OFF
ΔC_d	diffuse reflectivity difference between ON and OFF
A	total area of the device
R	attachment radius of the device
\vec{S}	sun direction vector
\vec{n}	surface normal vector of the device
\vec{r}	position of the device from center of gravity of overall spacecraft
h	z coordinate of vector r
h'	normalized vertical offset of the device ($=h/R$)
α	deflection angle of the device
β	distortion angle of the device
θ	phase of spin motion

θ_s	sun angle
p_0	momentum of sunlight per unit area
B_r	Lambertian coefficient
\vec{F}	instantaneous force vector applied to the device by solar radiation pressure
δ_1	phase of switching control
L	angular momentum accumulated during one spin motion
Ω	spin rate

Subscripts

b	body-fixed coordinate
on	a value when the device is ON
off	a value when the device is OFF
x	x coordinate of a vector
y	y coordinate of a vector
z	z coordinate of a vector

REFERENCES

- [1] Johnson, L., Young, R., Montgomery, E. and Alhorn, D., "Status of solar sail technology within NASA", *J. Adv. Space Res.*, Vol.48, Issue 11, pp.1687-1694, 2011, doi:10.1016/j.asr.2010.12.011
- [2] Kawaguchi, J., "A power sailer mission for a Jovian orbiter and Trojan asteroid flybys", COSPAR04-A-01655, Abstracts of 35th COSPAR Scientific Assembly, Paris, France, 18-25 July, 2004.
- [3] Funase, R., Shirasawa, Y., Mimasu, Y., Mori, O., et al., "On-orbit verification of fuel-free attitude control system for spinning solar sail utilizing solar radiation pressure", *J. Adv. Space Res.*, Vol.48, Issue 11, pp.1740-1746, 2011, doi:10.1016/j.asr.2011.02.022
- [4] Tsuda, Y., Mori, O., Funase, R., et al., "Flight Status of IKAROS Deep Space Solar Sail Demonstrator", Proceedings of 61th International Astronautical Congress, Prague, Czech Republic, IAC-10-A3.6.8, 2010.
- [5] Chishiki, Y., Mori, O., Sawada, H., Shirasawa, Y., et al., "Shape Estimation of IKAROS Membrane with Shape-from-Shading Method", Proceedings of 21st Workshop on JAXA Astrodynamics and Flight Mechanics, B-18, Sagamihara, Japan, 2011.
- [6] Matsunaga, S., Inagawa, S., Nishihara, T., et al., "On-Orbit Demonstration of Deployable Camera System for Solar Sail IKAROS", Proceedings of 28th International Symposium on Space Technology and Science, 2011-o-4-07v, Okinawa, Japan, 2011.
- [7] Tsuda, Y., Saiki, T., Mimasu, Y. and Funase, R., "Modeling of Attitude Dynamics for IKAROS Solar Sail Demonstrator", Proceedings of 21st AAS/AIAA Space Flight Mechanics Meeting, AAS11-112, Louisiana, USA, 2011.